Journal of Engineering and Applied Sciences 13 (19): 8081-8085, 2018
ISSN: 1816-949X

Improved Electrical Properties of PSi Photodetector by Embedding Ag

Warood Kream Alaarage
Department of Basic Science, College of Dentistry, University of Kufa, Kufa, Iraq

Abstract: The nanostructure silicon known as Porous Silicon (PSi) was prepared by the technique of electrochemical etching of crystalline silicon doped boron (p-type) with orientation (100) by using Teflon cell, HF with 40% concentration and Methanol with purity (99.9%) in (1:2) ratio at 9 mA/cm^2 current density and 13 min etching time. Ag nanoparticles was prepared by chemical reduction method. The structural, optical and electrical properties was investigated by using X-Ray Diffraction (XRD) Scanning Electron Microscope (SEM) Fourier Transform Infrared Spectroscopy (FTIR) and UV-visible spectrum. The electrical properties of Ag/PSi/c-Si/Al junction was studied by using dark I-V, illuminated I-V, C-V measurement and responsivity. The current study showed improvement in the electrical properties PSi photodetector after embedding AgNPs.

Key words: Porous Silicon (PSi), silver nanoparticles, XRD, SEM, FTIR, photodetector, responsivity

INTRODUCTION

Photodetectors are light sensors or other electromagnetic energy that alter light photons into electrical signal (Casalino, 2012). Si is a semiconductor with an indirect band gap, so that, it does not have photolumenesence, therefore, we convert Si from the bulk structure to nanostructure with direct and extensive band gap, excessive resistivity, large surface area to size ratio that is known a Porous Silicon (PSi). These valuable properties make (Psi) as attractive and promising material for superior Opto-electronic device fabrication (Ismail, 2010; Canham, 1990). Silver Nanoparticles (AgNPs) are very essential between the most broadly used metallic nanoparticles. They may be synthesized by different techniques including physical and chemical techniques, photochemical reduction, high temperature evaporation (Umoren *et al*., 2014) and electrochemical reduction (Algun and Arikan, 1999). In the synthesis of silver nanoparticles, top down and bottom up are the two essential synthesis methods for nanoparticles. Top down method can be seemed as a process starting with a bulk material after which breaking it into small dimension. Typical techniques consist of attrition, milling, lithography, mechanical and chemical manipulation apparatuses. The major advantages are universality and low fee. Even a soft organic material (e.g., grass) can be ground by means of first freezing it in liquid nitrogen (Yaakob *et al*., 2015). The major disadvantages are abnormal surface structure, polydispersity of the last particles and the introduction of several defects. The smaller the particle, the eviler is the infection (Muzamil *et al*., 2014).

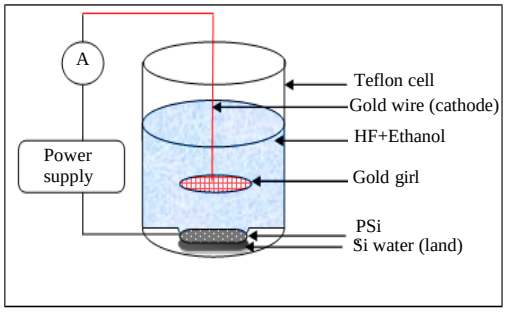

Fig. 1: The diagram of the electrochemical etching set-up

MATERIALS AND METHODS

Experiment procedure: PSi samples had been organized by the electrochemical etching process of boron doped p-type (100) oriented Si wafer ρ = 1-4 Ωcm HF with concentration (48%) and Methanol with purity (99.9%) in 1:2 ratio of current density (9) mA/cm^2 for 13min etching time at the room temperature in a Teflon single tank anodizing system such as shown in Fig. 1.

AgNPs was synthesed by the chemical reduction method by using NaOH as a reduction agent, 0.003 M of $AgNO_3$ was dissolved in methanol and heated to boil, then 7 mL of 1 % NaOH was added to the solution drop by drop,the solution were heated and mixed until color changed to pale yellow, then, removed from heater and it stirred until cooled to the room temperature.

In this research, the XRD (Shimadzu-XRD6000, Shimadzu Company/Japan) system was used for XRD measurements, the supply of X-ray radiation has been

Cu-kα radiation with 0.15406 nm wavelength, the tool has been operating at 40 kV and 30 mA emission current, the pattern is scanned from (20-60°). The SEM study has been preformed by using (Inspect S50/FEI company/Made in Netherlands) SEM prepared with EDX. The optical properties are examined via. (UV-VIS Spectrophotometer, Number: 21-1884-01-0041, Spectral Bandwidth: 2.00 nm) the scan range (190.00-500.00 nm), measure mode: Abs and interval: 2.00 nm, the absorbance of the prepared suspension can be assumed from the plot of the optical absorption against wavelength (nm). The (SHIMADZU- 8400S) Scan of the FTIR measurements are accomplished over the variety among (400-4000) cm^{-1} for the prepared sample. The electrical properties of nanostructure of Photodetector have been studied. All measurements had been accomplished in each dark room and daylight illumination. The electrical measurement convoluted current-Voltage (I-V) Capacitance-Voltage (C-V) measurements and responsivity.

RESULTS AND DISCUSSION

Xrd measurements: Figure 2 indicates X-ray diffraction of crystalline silicon and PSi samples. A strong peak of PSi at 9 mA/cm^2 current density shows a splitting peak at $2\theta = 33.5°$ orientated best alongside the 211 direction is perceived confirming the monocrystalline construction of the PSi layer which belongs to the 211 reflecting level of Si of cubic structure (according to ICDD N 1997 and 2011 JCPDS). The porous silicon peak intensity decreases while crystal size is reduced to the direction of nanometric scale and this attributed to the decrement of the crystalline size.

SEM investigation: The resulting structure was photographed by SEM is shown in Fig. 3, spherical its magnification (12165X) of AgNps. The particles are spherical and asymmetrical in form and randomly disbursed at the glass surface and this result agrees with (Shakir *et al*., 2017). The average diameter of the particles taken from Fig. 4 is 50 nm.

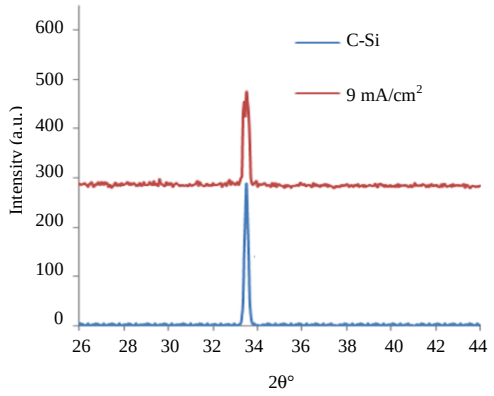

Fig. 2: XRD the spectra of (C-Si) and (PSi) sample for (13 min) etching time

UV-Vis analysis: The absorption characteristics can consider a useful tool to analyze nanomaterials. UV-Vis spectra can give valuable information about the evaluation of the degree of dispersion of AgNPs in methanol. Figure 4 shows the UV-Vis spectra of the colloidal of AgNPs. The strong peak around 240 nm corresponds to Ag absorbance peak, approved that Ag were successfully dispersed in methanol. The absorbance depends on the quantity of nanoparticles in methanol.

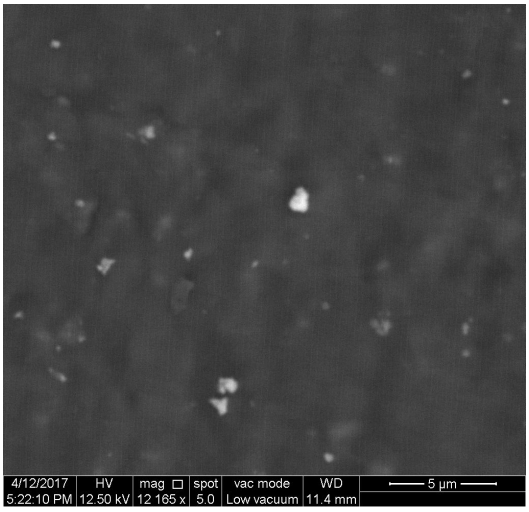

Fig. 3: SEM image of AgNPs

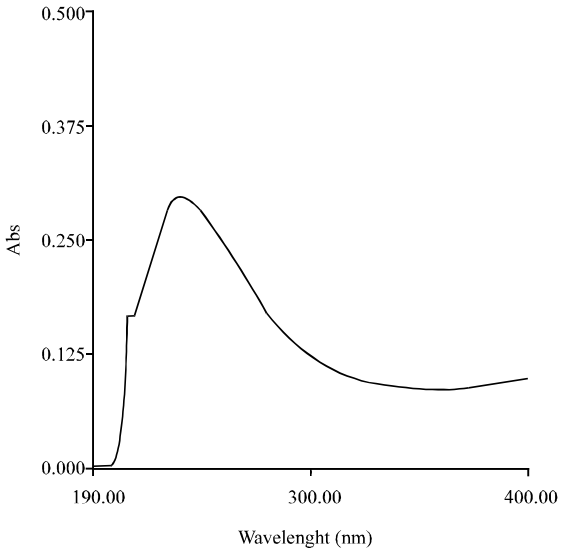

Fig. 4: UV-Vis absorbance spectra of AgNPs

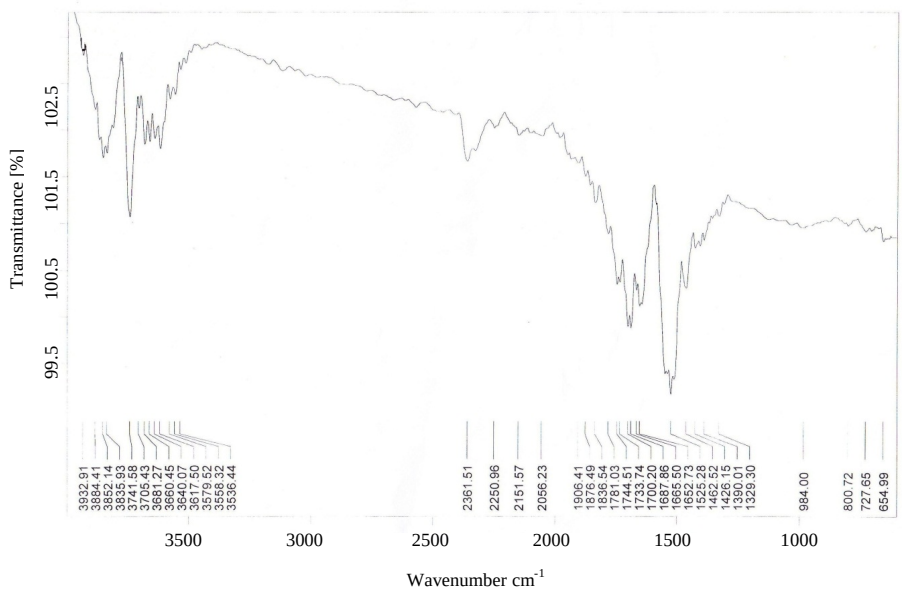

Fig. 5: FTIR absorption spectra of AgNPs

Adding, different secondary parameters like particle size, shape, dispersion, stability, etc., also are the keys in determining the absorption conduct.

FTIR measurements: Figure 5 shows the Fourier Transform Infrared (FTIR) spectroscopy of AgNPs. The peak of carboxylic acids is existent at 1652 and 1700 cm^{-1}, the carboxylic acid frequency variety is 1700-1300 cm^{-1} (Muzamil *et al*., 2014; Shakir *et al*., 2017). The peak at 2361 cm^{-1} refers to a primary amine group of protein (Phanjom and Ahmed, 2015; Vasquez-A *et al*., 2007; Lorusso *et al*., 2009; Alagumuthu and Kirubha, 2012). The peaks at 1457 cm^{-1} refer to amines and amino-methyl stretching groups of protein (Phanjom and Ahmed, 2015; Dian *et al*., 2013). The peak due to carbonyl stretch ~1744 cm^{-1} was detected when planes completed by the methyl ester group were analyzed (Mengistu *et al*., 2005).

Current-voltage characteristics: Figure 6 illustrates I-V current (forward and reverse) in the dark. The figure reveals that the dark forward current of Ag/PSi/c-si/Al higher than PSi/c-Si//Al and this mean that the sensitivity of the heterojunction increased after embedding AgNPs and this result agree with (Zhang, 2006).

Illuminated (I-V) characteristics: Figure 7 displays the reversed (I-V) characteristic of the devise measured under light intensity illumination (6424 $\mu w/cm^2$). It can be observed that the reverse current of PSi/c-Si/Al photodetector increased form 2498-4451 $\mu A/cm^2$ after

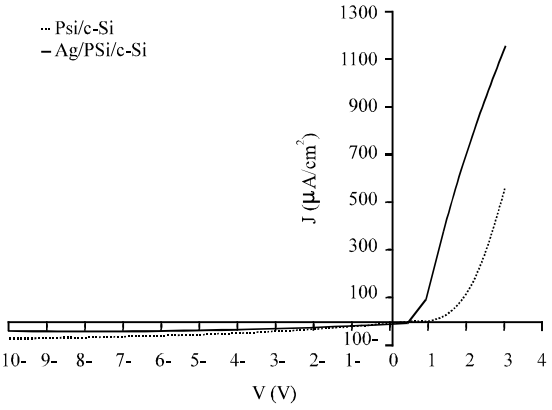

Fig. 6: Dark (I-V) characteristics of (Ag/PSi/c-Si) and (PSi/c-Si) photodetecter

embedding AgNPs and this attributed to the increment of the number of "electron-hole pairs" in the junction after embedding AgNPs.

Capacitance-Voltage measurements (C-V): Figure 8 exhibits a linear relationship between C^{-2} and reverse voltage and this mean that the junction was abrupt for both (Ag/PSi/c-Si) and (PSi/c-Si) junction. The bullions in a potential decrease after embedding AgNps and this mean that the electron required smaller power to remove from Ag layer to PSi layer and these expected to depend on the "Fermi-level" position in a conduction band at the high concentration of the carrier.

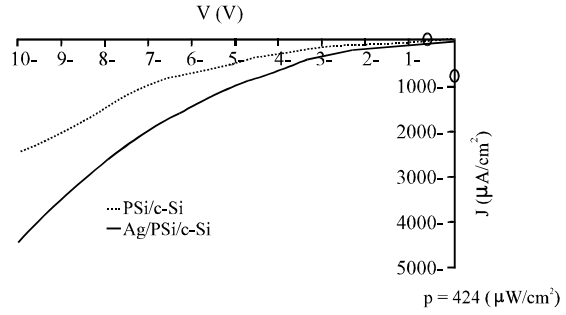

Fig. 7: Illuminated (I-V) characteristics of (Ag/PSi/c-Si) and (PSi/c-Si) photodetector

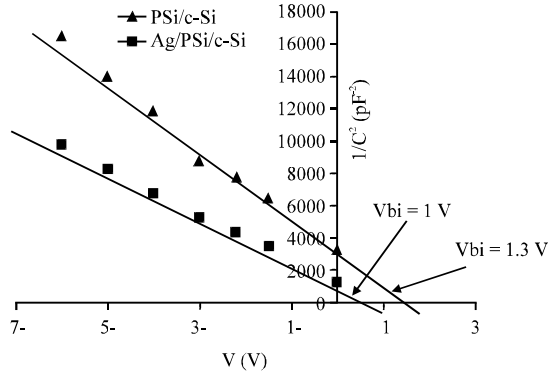

Fig. 8: (C^{-2}) vs. inverse voltage of (Ag/PSi/c-Si) and (PSi/c-Si) junction

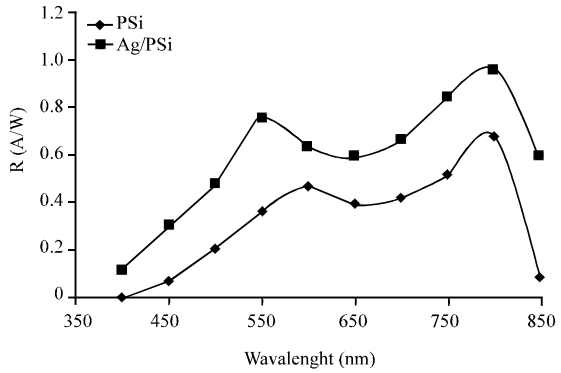

Fig. 9: Responsivity as a function of wavelength of AgNPs embedding (PSi/c-Si) photodetector

Responsivity: From Fig. 9 the spectral responsivity of (PSi/c-Si) photodetector was changed from 0.5-0.8 A/w by embedding AgNPs and this occur due to decrease of the barrier height. Figure 9 appearances that the spectral responsivity curve of AgNPs embedding (PSi/c-Si) contains of 2 peaks of response, the 1st peak was located at (600 nm) because of AgNPs absorption edge located in the visible region while the 2nd region was located at (825 nm) because of absorption edge of Si.

CONCLUSION

Ag/PSi/c-Si photodetector was fabricated and characterized without any oxidation or post-annealing. The porous layer construction was complete by XRD, SEM, FTIR and UV studies. The photodetector has good linearity characteristics and shows a good photoresponse in both UV and visible light. Embedding AgNPs to the PSi leads to increase the sensitivity of the heterojunction, increase the number of electron-hole pairs in the junction and decrease the billions in potential. The spectral responsivity of (PSi/c-Si) photodetector was changed from (0.5-0.8) A/w when embedding AgNPs and this occur due to decrease of the barrier height.

REFERENCES

Alagumuthu, G. and R. Kirubha, 2012. Synthesis and characterisation of silver nanoparticles in different medium. Open J. Synth. Theor. Appl., 1: 13-17.

Algun, G. and M.C. Arikan, 1999. An investigation of electrical properties of porous silicon. Turk. J. Phys., 23: 789-798.

Canham, L.T., 1990. Silicon quantum wire array fabrication by electrochemical and chemical dissolution of wafers. Applied Phys. Lett., 57: 1046-1048.

Casalino, M., 2012. Near-infrared sub-bandgap all-silicon photodetectors: A review. Intl. J. Opt. Appl., 2: 1-16.

Dian, J., M. Konecny, G. Broncova, M. Krondak and I. Matolinova, 2013. Electrochemical fabrication and characterization of porous silicon/polypyrrole composites and chemical sensing of organic vapors. Intl. J. Electrochem. Sci., 8: 1559-1572.

Ismail, R.A., 2010. Fabrication and characterization of photodetector based on porous silicon. J. Surf. Sci. Nanotech., 8: 388-391.

Lorusso, A., V. Nassisi, G. Congedo, N. Lovergine and L. Velardi et al., 2009. Pulsed plasma ion source to create Si nanocrystals in SiO2 substrates. Appl. Surf. Sci., 255: 5401-5404.

Mengistu, T.Z., L. DeSouza and S. Morin, 2015. Functionalized porous silicon surfaces as MALDI-MS substrates for protein identification studies. Chem. Commun., 45: 5659-5661.

Muzamil, M., N. Khalid, M.D. Aziz and S.A. Abbas, 2014. Synthesis of silver nanoparticles by silver salt reduction and its characterization. IOP. Conf. Ser. Mater. Sci. Eng., 60: 012034-012041.

Phanjom, P. and G. Ahmed, 2015. Biosynthesis of silver nanoparticles by Aspergillus oryzae (MTCC No. 1846) and its characterizations. Nanosci. Nanotechnol., 5: 14-21.

Shakir, A.A., A. ObaidHossain, W.M. Abdulridha and M.A. Mohammed, 2017. Toxipathological effect of silver nanoparticles on the brain and liver of albino rats. Intl. J. Chem. Tech. Res., 10: 624-629.

Umoren, S.A., I.B. Obot and Z.M. Gasem, 2014. Green synthesis cand characterization of silver nanoparticles using red apple (Malus domestica) fruit extract at room temperature. J. Mater. Environ. Sci., 5: 907-914.

Vasquez-A, M.A., G.A. Rodriguez, G. Garcia-Salgado, G. Romero-Paredes and R. Pena-Sierra, 2007. FTIR and photoluminescence studies of porous silicon layers oxidized in controlled water vapor conditions. Rev. Mex. de Fisica, 53: 431-435.

Yaakob, Y., M.Z.M. Yusop, C. Takahashi, M.S. Rosmi and G. Kalitaa et al., 2015. In situ transmission electron microscopy of Ag-incorporated carbon nanofibers: The effect of Ag nanoparticle size on graphene formation. RSC. Adv., 5: 5647-5651.

Zhang, G.X., 2006. Porous Silicon: Morphology and Formation Mechanisms. In: Modern Aspects of Electrochemistry, Vayenas, C., R.E. White and M.E. Gamboa-Adelco (Eds.). Springer, Boston, Massachusetts, ISBN:978-0-387-23371-0, pp: 65-133.